LATE QUATERNARY SEDIMENTATION IN TWO PHREATIC CAVES IN NORTHWERSTERN FLORIDA, USA: THE INFLUENCE OF CLIMATE VARIABILITY AND CAVE GEOMETRY

An Undergraduate Research Scholars Thesis

by

TYLER S. WINKLER

Submitted to Honors and Undergraduate Research
Texas A&M University
in partial fulfillment of the requirements for the designation as an

UNDERGRADUATE RESEARCH SCHOLAR

Approved by
Research Advisor: Dr. Peter J. van Hengstum

May 2015

Major: Marine Biology

TABLE OF CONTENTS

ABSTRACT

Late Quaternary sedimentation in two phreatic caves in northwestern Florida, USA: the influence of climate variability and cave geometry. (May 2015)

Tyler S. Winkler
Department of Marine Biology
Texas A&M University

Research Advisor: Dr. Peter J. van Hengstum
Department of Marine Sciences

Thick sediments have accumulated in many inland phreatic caves hosted by the Floridian Ocala limestone (USA), but the paleoenvironmental value of these sediments remains unknown. It is possible that phreatic cave sediments could provide proxy-based evidence for long-term hydrodynamics of the local aquifer. To test this hypothesis, several sediment cores were collected from two caves: Hole in the Wall Cave (HITW) and Twin Cave in Marianna, Florida (USA). The subsurface stratigraphy in both caves captures snapshots of the deglacial evolution of the Western Floridian aquifer, but radiocarbon dating indicates that a punctuated sediment supply and budget hampers the temporal continuity of the paleoenvironmental records. Sedimentation in both caves is dominated by fine-grained iron and manganese oxide and oxyhydroxide minerals. However, after 5600 calibrated years before present (Cal yrs BP), deposition in HITW switches to fine-grained organic matter, perhaps marking the onset of modern hydrologic conditions. In addition, a 40 cm unit of detrital organic matter deposited over ~100 years in Twin cave at 13,900 Cal yrs BP is perhaps related to a regional shift towards a warmer and wetter climate during the Bølling-Allerød warming at ~14,000 Cal yrs BP. These results indicate that sediments deposited in inland phreatic caves may provide paleohydrologic information if more continuous sedimentary records can be recovered.

CHAPTER I

INTRODUCTION

Scientific inquiry on the sedimentary deposits in caves and sinkholes has greatly expanded in the last several decades from the realization that cave and sinkhole sediments can preserve records of paleoceanography (Kitamura et al., 2007; Yamamoto et al., 2010; Yamamoto et al., 2009), tropical cyclone variability (Brandon et al., 2013; Denomee et al., 2014; Lane et al., 2011; van Hengstum et al., 2014), paleohydrology (Gabriel, 2009; van Hengstum et al., 2010), millennial-scale terrestrial-oceanic climatic connectivity (Grimm et al., 1993), sea level proxies (Gabriel et al., 2009; Kovacs et al., 2013), glacial-interglacial oscillations (Larsen and Mangerud, 1989), and precipitation variability (Polk et al., 2013; Wurster et al., 2008). Despite the known significance of cave and sinkhole sediments to paleoclimate research, our understanding of cave sedimentary emplacement mechanisms and their facies associations lags behind.

In general, cave sedimentation is dependent upon many factors, such as regional hydrography, the geometry of cave passages, proximity to the ocean and tidal action. Cave sedimentary units themselves are often divided into either allochthonous sediment transported into the cave through fluvial, aeolian, or marine processes; or autochthonous formed within the cave itself (Bosch and White, 2007; Ford and Williams, 1989; White, 2007). Allochthonous sediments are dependent upon regional geology and local weathering processes (Bosch and White, 2007; Fornós et al., 2009; White, 2007). Autochthonous clastic sediments include fluvial and gravitational breakdown products, insoluble clasts such as chert and silicified fossil fragments eroded out of the surrounding bedrock, and in situ organic deposits like guano (White, 2007). The origins and

mineralogy of autochthonous chemical sediments are diverse and strongly influenced by regional geochemistry and hydrologic processes. Chemical sediments are deposited in relation to three different processes: 1) dissolution and precipitation of minerals during hypogenic speleogenesis; 2) minerals precipitating at the interface of bedrock and aqueous water in littoral conditions, and 3) evaporitic and redox minerals that precipitate during vadose cave conditions (Onac et al., 2014; Onac et al., 1997; White, 2007).

The presence of standing or flowing water within conduits remains an important factor controlling cave sedimentation. As such, the proximity of a specific cave to the coastline, the relative impact of sea-level change, and oceanographic variability on base-level change in the cave are all important variables impacting cave sedimentation . For riverine systems on siliciclastic coastlines, base level refers to the elevation of the water table and represents the lowest possible point to which the river can erode. Infiltrating water on carbonate landscapes also seeks base level, but the high porosity of carbonates can typically allow for the direct infiltration of meteoric water into the subsurface to reach base level and ultimately enter the phreatic zone. Cave conduits for both inland and coastal caves can be positioned in the vadose (unsaturated) zones, phreatic (saturated) zones, or both, depending upon the stratigraphic position of base level. On geologic timescales, of course, the elevation of base level is not constant and can change in response to regional geologic variability, climate variations, or sea-level change (Florea et al., 2007; Gulley et al., 2012).

Although slightly subjective, it has been suggested that coastal caves are those with a measurable influence of marine tidal action on the regional aquifer (Guilcher, 1988; van Hengstum et al.,

2015), wherein the position of base level is concomitantly linked to glacioestatic sea-level variability. In contrast, further inland base level is more strongly dependent upon local hydrologic and geologic variables (Guilcher, 1988; van Hengstum et al., 2015). The sediment in inland vadose caves is commonly characterized by fluvial-like depositional processes, and the texture ranges from cobble- to boulder-sized clastic sediments (Kyrle, 1923; Trombe and Fage, 1952; Bosch and White, 2007), with primary sedimentary structures varying from massive to laminated deposits (Bull, 1981). In contrast, sediments deposited in phreatic (submerged) coastal caves tends to be dominated by carbonates, organic matter, and ferromanganese sedimentary facies (Fornós et al., 2009; van Hengstum et al., 2010; van Hengstum et al., 2011). However, sedimentary facies and depositional environments within phreatic inland caves remain unknown.

The objectives of this study are to: (i) determine the subsurface stratigraphy in an inland phreatic cave system; (ii) investigate the temporal relationships between stratigraphic variability and aquifer hydrodynamics; (iii) ascertain any possible relationships between stratigraphic variability and regional climate dynamics.

Study site

Hole in the Wall (HITW) Cave (N 30.78327º, W 085.15618º ± 3 m) and Twin Cave (N 30.78691º, W 085.14494º ± 3 m) in Jackson County, Florida are located ~300 m apart within the same surface stream system, Merritts Mill Pond (Fig. 1). These caves are located in within Marianna Lowlands physiographic providence, a region that formed as a result of uplift created by the Chattahoochee Anticline (Schmidt, 1988). Both systems formed in the Ocala Limestone which was deposited in the early Oligocene epoch (Cooke, 1939, 1945; Puri, 1964; Schmidt,

1988; Survey et al., 2001; White, 1970). The Ocala Limestone is defined by a yellow to white, massive, porous, and often silicified limestone that is rich in remnant echinoid, mollusks, bryozoan, and foraminifera fossils (Cooke, 1945; McKinney and Zachos, 1986; Schmidt, 1984; Schmidt, 1988). This region is approximately 30 m lower than the surrounding area and is heavily karstified as a result of continuous fluctuations in sea level over time have impacted regional hydrographic conditions including groundwater levels and stream gradients (Cooke, 1945; Schmidt, 1988).

Merritts Mill Pond is a 1.093 km^2 surface stream water feature that was once the upper portion of

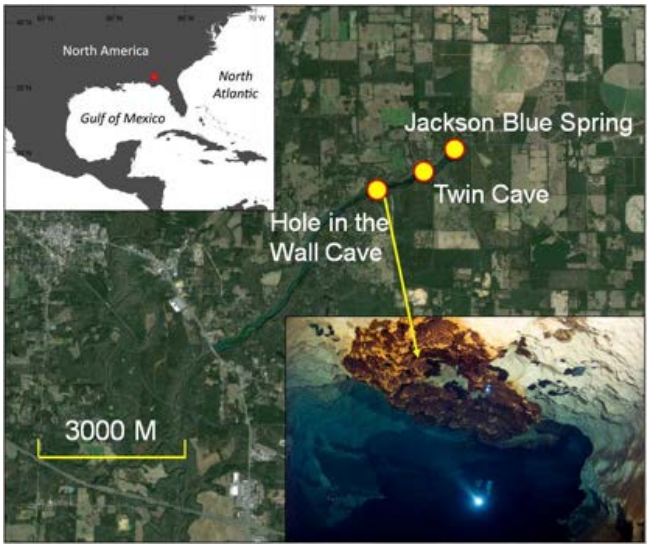

Figure 1: Location of sampling sites in Meritt's Mill Pond in Jackson County, FL.

a spring run fed by meteoric groundwater emerging from Jackson Blue Spring (Dodson, 2013). In 1920, Merritts Mill pond was expanded to its current size after a dam and weir structure was constructed at U.S. Highway 90 (Dodson, 2013). Based on observations made while in the site, modern sediment accumulations in Merritts Mill Pond are minimal with the underlying bedrock exposed across much of the bottom of the stream.

It has been suggested that many inland phreatic caves in the Northern Floridian aquifer have oscillated between phreatic and vadose phases in response to Quaternary glacioeustacy and its concomitant effect on the regional water table (Florea et al., 2007; Gulley et al., 2012; LeGrand and Stringfield, 1966; Zarikian et al., 2005). Caves in the same region as HITW Cave and Twin Cave, such as the Devil's Cave System, are thought to have formed as entranceless voids within the surrounding bedrock as a result of CO_2 diffusion into the lower water table during quaternary glacial periods (Gulley et al., 2012). These caves would have existed in the vadose zone during Quaternary sea-level low stands, but sea-level rise during interglacials would have forced regional base-level rise to create the modern phreatic zone characterized by the modern upper Floridian aquifer (Florea et al., 2007; Gulley et al., 2014; Gulley et al., 2012).

Numerous studies have utilized sedimentary records to demonstrate that the Floridian aquifer is impacted by both regional and global climate variability (Alverez Zarikian et al., 2005; Hansen, 1990; Opsahl et al., 2005; Watts et al., 1992). Based on the successful utilization of sediments in coastal phreatic caves as archives of long-term paleohydrological changes (Fornós et al., 2009; van Hengstum et al., 2009; van Hengstum et al., 2011) as well as studies linking modern inland phreatic cave sediments to measurable hydrodynamic oscillations (Opsahl et al., 2005), it is possible that sediments from inland phreatic caves are impacted the behavior of surface stream and groundwater sources and can be utilized as a long-term record of regional paleohydrologic change.

CHAPTER II

METHODS

A coring survey was completed in May 2011 and July 2014 that produced 11 push cores from the underwater caves: five cores from HITW Cave and six from Twin Cave (Figs. 2, 3). Coring operations were completed using advanced technical cave diving procedures, following safety protocols exceeding those outlined by the American Academic of Underwater Sciences. To collect the sediment cores, a 5 or 8 cm diameter and 2.4 m length transparent polycarbonate pipe was vertically inserted into the sediment, and thereafter withdrawn after creating suction to retain the stratigraphy. Coring sites were separated by approximately 60 meters of horizontal cave passage at water depths ranging from 15 to 30 m below the modern water table. After extraction, cores were transported back to the laboratory where they were split lengthwise, described and stored at 4ºC until further sedimentary processing. Also while in the field in July 2014, hydrographic parameters including depth (± 0.04 m), temperature (± 0.01°C), conductivity (± 0.001 mS/cm), pH (± 0.2 pH units), and dissolved oxygen (± 0.1 mg/L) were measured using a YSI EXO1 Water Quality Sonde.

Figure 2: Coring locations in HITW Cave.

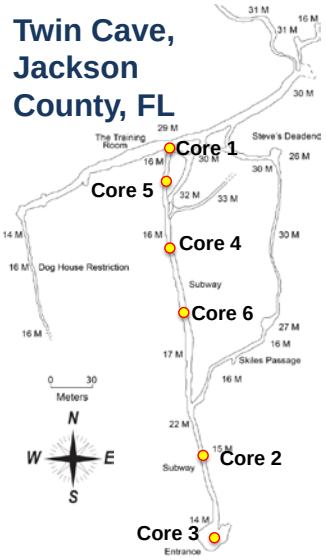

Figure 3: Coring locations in Twin Cave.

Visual sedimentary descriptions

Collected sediment cores were split and visually described in the laboratory. During the core description process, the 2009 Year Revised- 2012 Production of the *Munsell Soil Color Book* was used to describe the color of broad scale sedimentary units as well as all distinct sedimentary laminations. Any visible sedimentary textural variability or changes in organic matter content were also noted. High resolution photography of all sediment cores was also completed at this time in order to document the sedimentary record visually in a pristine state. These visual descriptions were utilized in making decisions on where to prioritize sampling for radiocarbon dating and mineralogical analyses.

Textural and organic matter variability

Coarse fraction variability was investigated using a modified loss on ignition procedure (Brown et al., 2013) to determine the mass of coarse grained sediment (<63 μm) per cm^3 of sediment. 2.5 cm^3 of sediment was sampled at contiguous 1 cm intervals throughout all 11 cores. Sediment was sieved over 63 μm mesh, emptied into ceramic crucibles, and dried in an oven 80ºC for 12 hours or until dry. After the dry sediment and the crucible were weighed, the sediment and crucibles were placed in a furnace and burned at 550ºC for 4.5 hours to ash organic constituents. The crucible and remaining sediment residue were then re-weighed to determine a final mass. The mass of the empty crucibles were subtracted from the final mass of the crucible and the burned sediment in order to determine the final mass of the coarse grained sediment without organic matter. This mass was then multiplied by 1000 and divided by 2.5 to determine mg of coarse grained sediment per cm^3. Equation (1) was used to calculate mg coarse sediment per cm^3:

$$\text{mg Coarse grained sediment per cm}^3 = \frac{\text{Mass of dry sediment after burn} * 1000}{2.5} \quad (1)$$

Loss on ignition analysis was also implemented in order to observe downcore variations in bulk organic matter (Heiri et al., 2001). Sediment was sampled at 1cm increments throughout all cores and transferred into a ceramic crucible and dried in an oven 80ºC for 12 hours or until dry. After the dry sediment and the crucible were weighed, the sediment and crucibles were placed in a furnace and burned at 550ºC for 4.5 hours. The crucible and the burned sediment were weighed again to determine a final mass from which the mass of the empty crucibles were subtracted to determine the final mass of the coarse grained sediment without organic matter. The percentage of organic matter (% OM) in the sample was calculated using equation (2):

$$\% \text{ OM } = \frac{\text{Mass of dry sediment before burn} - \text{Mass of dry sediment after burn}}{\text{Mass of dry sediment before burn}} * 100 \quad (2)$$

Mineralogy and trace metals

A total of 19 sediment sub-samples from specific sedimentary units in HITW-C1 and C2 as well as TWIN-C1, C4, C5, and C6 were selected for detailed mineralogical investigation of the fine-grained sediments via X-Ray Diffraction (XRD) analysis. Before XRD analysis, sediment was wet sieved over a 45 μm mesh to concentrate silt- and clay-sized sediment particles, which were then desiccated overnight aluminum drying pans in an oven heated to 80ºC. Desiccated sediment residues were then homogenized into a fine powder with a mortar and pestle. For XRD analysis, a sub-sample of each sediment residue was placed in the sample holder of a two circle goniometer, and enclosed in a radiation safety enclosure. The X-ray source was a 2.2 kW Cu X-ray tube maintained at an operating current of 40 kV and 40 mA. The X-ray optics was the standard Bragg-Brentano para-focusing mode with the X-ray diverging from a DS slit (1 mm) at the tube to strike the sample and then converging at a position sensitive X-ray detector (Lynx-Eye, Bruker-AXS). The two circle 250 mm diameter goniometer was computer controlled with

independent stepper motors and optical encoders for the Θ and 2Θ circles with the smallest angular step size 0.0001º 2Θ. The software suit for data collection and evaluation was Windows based. Data was collected using the automated COMMANDER program by employing a DQL file. All data was analyzed using the program EVA to match experimental diffraction patterns with reference diffraction patterns from the 2005 International Center for Diffraction Data (ICDD) material identification database in order to determine the precise mineralogy of the experimental sample.

Of the 19 sediment samples that were analyzed using XRD, the first ten (S1-S10) were subjected to additional analysis using Fourier Transform Infrared Spectroscopy (FTIR) to further confirm the sediment mineralogy. Extracted sediment samples were analyzed using the Varian Excalibur 3100 FTIR spectrometer by placing the sample on a diamond stage plate and transmitting infrared light between wavenumbers 500 and 4000 cm^{-1} through the sample. The percent transmittance was collected and graphed in VarianPro software. The peaks of spectrograph correlate to specific chemical bonds within the mineral, and were identified by aligning the experimental values with reference values from the literature.

To understand qualitative sedimentary trace metal variability, HITW-C1 was scanned using an ITRAX X-ray fluorescence (XRF) scanner. Using a Mo X-ray source, the intensity of emitted fluorescence of 38 elements were recorded at 0.25 cm intervals throughout the core.

Radiocarbon dating

Table 1: Radiocarbon Dates

Index No.	Lab number	Core	Core depth (cm)	Material dated	Conventional ^{14}C age (BP)	$\delta^{13}C$ (‰)	2σ calendar ages in yrs. BP (probability)	1σ calendar ages in yrs. BP (probability)	Calibrated 2σ age (yrs. BP)
1	OS-109437	HITW-C1	36 to 37	bulk organics	4920 ± 30	-29.1	5596-5666 (0.836) 5671-5714 (0.164)	5605-5655 (1)	5630 ± 30
2	BETA-390615	HITW-C2	0-1	bulk organics	3320 ± 30	-29.7	3470-3625 (1)	3486-3536 (0.547) 3549-3585 (0.453)	3550 ± 75
3	OS-109438	HITW-C2	34 to 35	bulk organics	4780 ± 30	-29.15	5468-5590 (1)	5479-5536 (0.871) 5577-5585 (0.129)	5530 ± 60
4	OS-109439	TWIN-C1	4.5-5.5	bulk organics	3560 ± 25	-28.39	3728-3748 (0.042) 3764-3792 (0.066) 3823-3926 (0.879) 3949-3959 (0.012)	3834-3889 (1)	3920 ± 50
5	BETA-390616	TWIN-C1	0-1	bulk organics	4490 ± 30	-28.2	5038-5297 (1)	5052-5077 (0.152) 5104-5134 (0.182) 5162-5195 (0.204) 5206-5280 (0.463)	5170 ± 130
6	OS-109440	TWIN-C1	23-24	bulk organics	12100 ± 45	-31.37	13787-14105 (1)	13853-13912 (0.288) 13921-14045 (0.712)	13950 ± 160
7	OS-109441	TWIN-C1	66.5-67.5	bulk organics	12000 ± 50	-29.49	13738-14013 (1)	13764-13872 (0.730) 13878-13927 (0.270)	13930 ± 190

Seven samples of bulk organic matter from TWIN-C1, HITW-C1, and HITW-C2 were submitted for Accelerator Mass Spectrometry radiocarbon dating (Table 1). Final conventional radiocarbon dates were calibrated with IntCal13 (Reimer et al., 2013) using the freeware CALIB 7.1 software

Lithofacies identification

In order to accurately describe the broad characteristics organic matter composition and textural variability of sediments in a specific lithofacies, the stratigraphy was divided into coherent lithofacies based on visual sedimentary character, textural variability, organic matter content, mineralogy, and age based radiocarbon dating. Once lithofacies divisions were established, it was necessary to remove statistical outliers caused by standard error in laboratory methods or isolated sedimentological phenomenal in order to observe accurate trends in the mean values, standard deviation, and modal distribution of LOI and coarse fraction variability data. The modified Thompson tau method was utilized to determine outliers in these datasets as this technique provides an objective, statistically derived rejection zone based on the mean value and standard deviation of a specific dataset.

CHAPTER III

RESULTS

The sediment accumulation in the surveyed areas of HITW Cave are significant, with sedimentary successions exceeding 2.4 m at each of the coring locations. Five cores were taken in HITW Cave with ultimate sediment recovery ranging from 90 to 166 cm after compression and de-watering (Table 2; Fig. 4). The depth of the bedrock was not found during the coring survey of HITW cave, making it difficult to determine how accumulation depths vary in in relation to proximity to the cave entrance. In contrast, sediment accumulation in Twin Cave was more limited as bedrock was reached on all coring drives, with the ultimate sedimentary recovery ranging in lengths from 56.5 to 113 cm for the cores (Table 3, Fig. 4). In general, sediment accumulations in Twin Cave appear to increase with increasing penetration into the cave, except TWIN-C5. The sediment in both caves could be categorized into one of six discrete lithofacies, which are described in further detail below.

Table 2: Core location, water depth, and sediment recovery

Core	Cave Penetration (m)	Water Depth (m)	Sediment Recovery (cm)	Basement reached (Y/N)
HITW-C1	15	26	157	N
HITW-C2	50	26	166	N
HITW-C3	274	30	111.5	Y
HITW-C4	244	28	150.5	N
HITW-C5	137	26	88	Y
TWIN-C1	250	28	113	N
TWIN-C2	60	51	60	Y
TWIN-C3	10	46	56.5	Y
TWIN-C4	200	16	82	Y
TWIN-C5	230	16	68	Y
TWIN-C6	150	16	78	Y

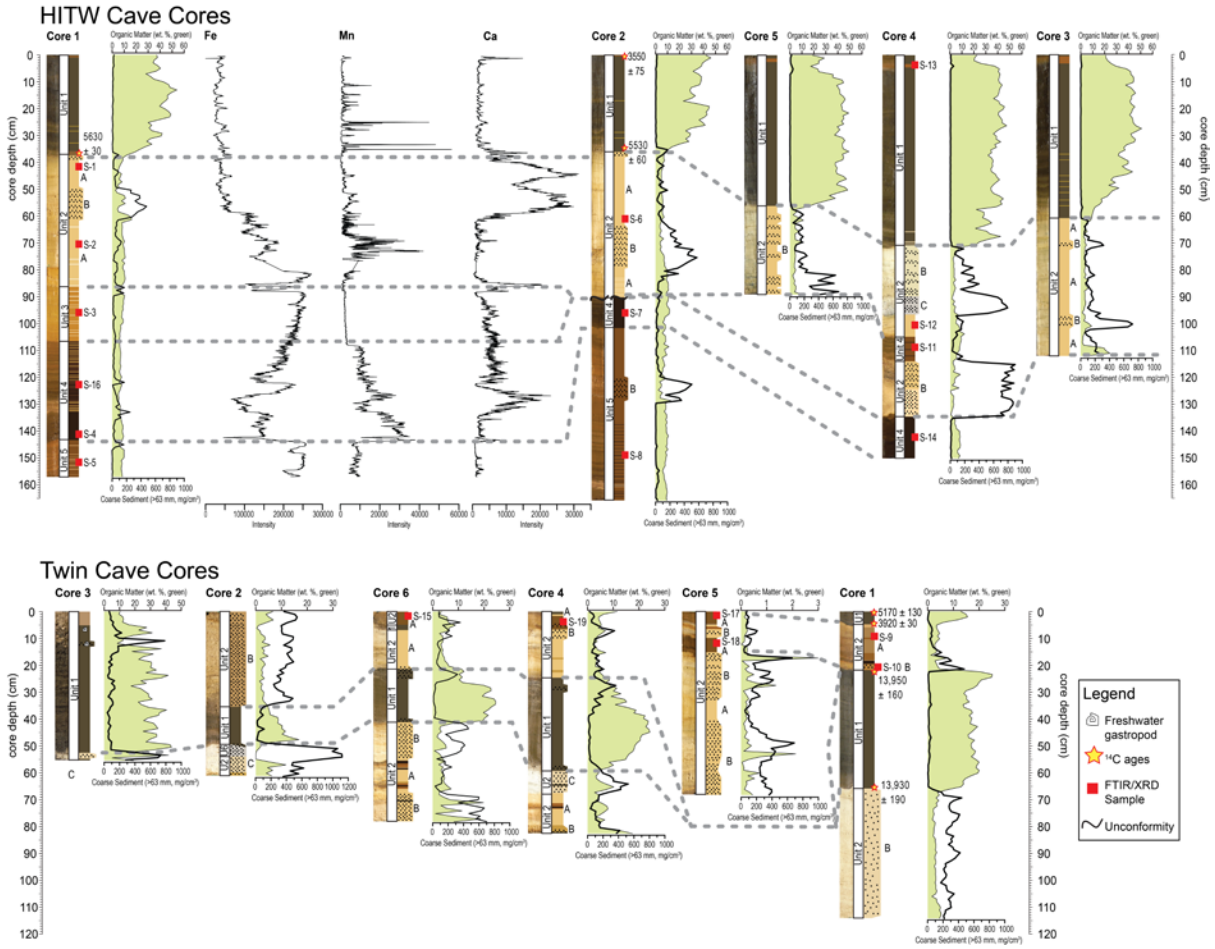

Figure 4: Stratigraphic variability (core logs and photographs), and correlation of lithofacies between sediment cores from Hole in the Wall and Twin Caves. Lithofacies divisions have been indicated in the diagram as well as the location for discrete sediment samples used for XRD and FTIR analysis and radiocarbon dating. Bulk organic content (wt. %) is represented by the green area to the right of each core. The mass of coarse sediment (>63 µm) per cubic cm throughout each core is indicated by the thick black plot to the right of each core. Trace metal abundances (Fe, Mn, Ca) on HITW-C1 from XRF analysis.

Lithofacies

Unit 1: Bulk organic matter

Unit 1 is present in both HITW Cave and Twin Cave and is dominated by bulk organic matter. However, its stratigraphic position downcore, horizontal distribution, and timing of accumulation varies both within and between each cave. This lithofacies had the highest average organic matter content (29% ± 11%) of all the units observed, although the complete distribution of all

samples measured (n = 424) was roughly bimodal with a weak peak at 17% to 20% organic matter and another at 40-45% organic matter. Visually, this unit can be described as 'black' (Munsell color: 10YR 2/1) with occasional 'brownish yellow' (Munsell color: 10YR 6/8) laminations. The unit was primarily fine-grained, except at the entrance to Twin Cave in TWIN-C3, which was dominated by coarse-grained organic fragments and freshwater gastropod shells (Fig. 4, 5). Rare horizons of coarse sediment (e.g., 35 to 36 cm in HITW-C2) were present within the unit. These horizons were primarily made up of Eocene-aged fossil material (e.g., echinoid spines, marine foraminifera), which most likely eroded out of the host limestone bedrock. As such, the average content of coarse sediment (>63 μm) fraction in Unit 1 was 22 mg/cm^3 ± 33, but was less than 20 mg/cm^3 in 71.5% of the samples.

The metal oxide abundance in unit was generally low based on XRF elemental analysis of HITW-C1. Unit 1 is characterized by low iron, manganese, and calcium abundance overall, but with narrow spikes in manganese and iron abundance that are correlated to the appearance of 'brownish yellow' (10YR 6/8) downcore laminations (e.g., 26 to 37 cm, HITW-C1). A 1 to 3 cm wide 'yellowish red' (5YR 4/6) horizon appeared near the sediment-water interface of all of the cores taken in HITW Cave (Fig. 4). XRD analysis of sediment from this horizon (Sample: 3 to 4 cm, HITW-C4) indicated that metal oxide minerals goethite ($Fe_3(O)OH$) and birnessite ($(Na_{0.3}Ca_{0.1}K_{0.1})(Mn)_2O_4$) were present in this sediment along with quartz (SiO_2) and calcite ($CaCO_3$) (Fig. 6).

Unit 1 sediments can be further subdivided into two distinct units based on the radiocarbon age and detailed textural variability. Unit 1A sediments were deposited from 5630 ± 30 to 3550 ± 75

Cal yrs BP, and the sedimentary matrix was characterized by clay- to silt-sized organic matter fragments. In contrast, Unit 1B was deposited in a much narrower age range of 13,950 ± 160 to 13,930 ± 190 Cal yrs BP and the sedimentary matrix included more-intact, leafy organic matter particles in an overall fine-grained matrix of bulk organic matter.

Unit 2: Texturally-variable carbonate

This is the most widespread, texturally-variable and mineralogical diverse lithofacies, which occurs in both HITW Cave and Twin Cave. XRF elemental analysis of Unit 2 in HITW-C1 indicates that calcium is a major elemental component throughout most of Unit 2 sediments, with varying levels of iron and manganese. Based on XRD (Fig. 6) and FTIR (Fig. 7) analyses, the mineralogy in Unit 2 was more crystalline that the other units, with calcite ($CaCO_3$) and quartz (SiO_2) being the most prevalent minerals. Other iron and manganese oxide and oxyhydroxide minerals were also detected (Fig. 6, 7; Table 3), such as goethite ($Fe_3(O)OH$), magnetite (Fe_3O_4), and trace amounts of kaolinite ($Al_2Si_2O_5(OH)_4$). In general, Unit 2 contains an average organic matter content of 4% ± 3 which is the 2nd lowest average of all the recovered lithofacies. Unit 2 has the second highest mean coarse sediment (>63 µm) fraction at 209 g/cm^3 ± 146 with 54.76% of sediment samples (n = 494) from this unit occurring in the range of 40 to 200 g/cm^3, which clearly depicts the textural heterogeneity in the unit.

As a result of the considerable textural variability, Unit 2 was subdivided into Units 2A, 2B, and 2C based on texture, color, and some mineral variability. Unit 2A is dominated by silts and clays and with color ranging from ‘yellow’ (Munsell color: 10YR 8/6) to ‘strong brown’ (Munsell color: 7.5YR 4/6). In contrast, Unit 2B is much more coarse-grained as it contains abundant

Eocene-aged marine fossils including an ichthyoid tooth found at 86 cm in HITW-C4 (Fig. 5) in a fine-grained matrix. Unit 2B can range in color from ‘very pale brown’ (Munsell color: 10YR 8/3) to ‘brownish yellow’ (Munsell color: 10YR 6/8). A third subsection, Unit 2C, occurs in TWIN-C2, TWIN-C4, and HITW-C4. This subsection is characterized by very coarse, rounded grains of ‘white’ (Munsell color: 10YR _/1) calcium carbonate particulate with ‘black’ (Munsell color: 10YR 2/1) sand-sized clasts that are likely eroded chert nodules. XRF elemental analysis of Unit 2 in HITW-C1 shows that Unit 2A (Unit 2B) had a higher (lower) abundance of iron and manganese with lower (higher) Ca abundance (Fig. 4).

Unit 3: Fine-grained iron-rich lithofacies

Unit 3 is a generally homogenous lithofacies dominated by iron-based particles (according to XRF analysis; Fig. 4) in a fine-grain sedimentary in matrix. In general, Unit 3 sediments are ‘reddish yellow’ (Munsell Color: 7.5YR 6/8) in color which can be attributed to the richness of Fe in the sediment. XRD (Fig. 6) and FTIR (Fig. 7) analyses on a single sediment sample taken from HITW-C1 revealed that goethite ($Fe_3(O)OH$), magnetite (Fe_3O_4), calcite ($CaCO_3$), and quartz (SiO_2) minerals are the only observable minerals in this unit. ‘Yellow’ (10YR 7/8) clayey laminations occur frequently throughout this lithofacies and appear to correlate to increased levels of calcium in the sediment (according to XRF scan of HITW-C1; Fig. 4). This lithofacies contains very little organic matter, with a mean composition of 8% ± 1%. Occasional coarse sedimentary horizons that are made up of Eocene aged echinoid fossils occur within the fine grained matrix at varying intervals. The average coarse sediment (>63 μm) fraction of this unit is 26 g/cm^3 ± 12 with 52.38% of samples (n = 21) from this unit having a coarse sediment fraction in the range of 15 to 21 g/cm^3. This unit only occurs in HITW-C1.

Unit 4: Fine-grained iron- and manganese-rich sediment

Unit 4 sediments are generally very fine 'dark brown' (7.5YR 2.5/2) clays and silts. XRF elemental analysis of HITW-C1 indicates that this unit is rich in manganese as well as iron (Fig. 4). XRD and FTIR analyses on five Unit 4 sediment samples taken from HITW-C1, HITW-C2, and HITW-C3 show that manganese oxide minerals such as birnessite ($(Na_{0.3}Ca_{0.1}K_{0.1})(Mn)_2O_4$), jacobsite ($MnFe_2O_4$), and ramsdellite ($MnO_2$) form a significant portion of the sediment along with the goethite ($Fe_3(O)OH$), calcite ($CaCO_3$), and quartz (SiO_2) minerals that are found in almost every other lithofacies (Fig. 6, 7; Table 3). 'Yellow' (10YR 7/8) and 'black' (10YR 2/1)fine-grained laminations appear throughout most of Unit 4 sediments and, similarly to Unit 3 laminations, appear to correlate to increased levels of calcium in the sediment (according to XRF scan of HITW-C1; Fig. 4). Unit 4 sediments a have a mean organic matter composition of 7% ± 1. Though Unit 4 sediments are primarily massive silts and clays, this unit has a mean coarse sediment (>63 µm) fraction value of 29 g/cm^3 ± 22 (Fig. 4) resulting from occasional coarse horizons of Eocene aged marine echinoid fossils (Fig. 5) that appear sporadically throughout this unit.

Unit 5: Laminated iron-oxyhydroxide lithofacies

Unit 5 sediments only occur in HITW-C1 and HITW-C2 and are primarily composed of 'dark reddish brown' (5YR 3/4) massive silts and clays in a matrix. This lithofacies was visually striking, with a distinctive rust color. Based on the XRF elemental analysis from HITW-C1, this is the most iron-rich, yet manganese and calcium deficient units recovered (Fig. 4). Detailed XRD and FTIR analysis of two sediment samples from this unit in HITW-C1 and HITW-C2 indicate that goethite ($Fe_3(O)OH$) is the dominant mineral in this lithofacies (Fig. 6, 7), with

lesser amounts of calcite ($CaCO_3$) and quartz (SiO_2)(Fig. 6, 7). This unit is the most laminated of all of the lithofacies observed having ‘dark brown’ (7.5YR 2.5/3) clayey laminations that appear to correlate to increases in manganese as well as ‘brownish yellow’ (10YR 6/8) laminations that appear to correlate to an increase in calcium (Fig. 4). Organic matter content in this lithofacies is very low, having a mean value of 8 % ± 1%. This unit has a mean coarse sediment (>63 µm) fraction of 18 g/cm^3 ± 28 g/cm^3. A more accurate metric for describing the overall coarse sediment (>63 µm) fraction variability in this lithofacies is provided by the modal frequency in which 61.76% of the samples (*n* = 68) have a coarse sediment (>63 µm) fraction less than 10 g/cm^3.

Unit 5 sediments can be further subdivided into the subunits Unit 5A and Unit 5B based upon variability in texture. Unit 5A is the predominant subunit in this lithofacies and is composed entirely of clays silts in a matrix. Unit 5B is composed of coarse sediments made up of Eocene aged marine echinoid fossils (Fig. 5) in a fine grained matrix. The sharp contrast between the texture of these subunits is responsible for the high standard deviation value (± 28 g/cm^3) in the overall coarse sediment (>63 µm) fraction of this lithofacies.

Unit 6: Quartz sand

Unit 6 is a very coarse, very well sorted unit that appears to be made up entirely of ‘white’ (10YR 8/1). This lithofacies is only present in TWIN-C2 at 49 to 54 cm, just before the onset of the deposition of the gyttja lithofacies (Unit 1). Sediments from this unit were too coarse to be analyzed using XRD and FTIR methods; however, there was no significant change in the mass of a sample of Unit 6 sediment after it had been placed in HCl, indicating that the sediment is likely

dominated by a silica mineral such as quartz (SiO_2). As shown by LOI analysis (Fig. 4), sediment accumulation in this lithofacies has little to no organic matter with a mean composition of >1% ± 1. This lithofacies has the highest mean coarse sediment (>63 μm) fraction of all of the observed lithofacies with a value of 1074 g/cm^3 ± 59. Unlike all of the other lithofacies, Unit 6 had no visible fossil material.

Figure 5: Photographs of some of the more common fossils deposited in HITW Cave and Twin Cave sediments.

Table 3: Lithofacies Characteristics

Sed. Unit	General Texture	Coarse Sed. (>63 µm)	Average OM Content %	Fossils	Munsell Color	Mineralogy
1	A) Very fine (lower) Very well sorted B) More intact, leaf-like organic matter in a fine grained bulk organic matter matrix	**Average**: 22 ± 33g/cm^3 **Modal Freq.**: 71.53% <20 g/cm^3 (n = 424)	30% ± 12	Rare freshwater gastropod shells and Eocene aged Echinoid spines	*General*: 'Black' (10YR 2/1) *Laminations*: Top: 'Yellowish red' (5YR 4/6 Downcore: 'Brownish yellow' (10YR 6/8)	Bulk organic matter Top: Goethite (Fe(O)OH) Birnessite ((Na0.3Ca0.1K0.1)(Mn)$_2$O$_4$) Calcite ($CaCO_3$) Quartz low (SiO_2)
2	A) Very fine (lower) B) Very coarse (lower)-angular grains C) Very coarse (lower)-rounded grains	**Average**: 209 ± 146 g/cm^3 **Modal Freq.**: 54.76% 40 g/cm^3< x < 200 g/cm^3 (n = 494)	4% ± 3	Echinoderm spines and shell fragments dating to the Eocene	A) *General*: Varies from 'Yellow' (10YR 8/6) to 'Strong brown' (Munsell color: 7.5YR 4/6) B) *General*: 'brownish yellow' (10YR 6/8) C) *General*: 'White' (10YR _/1) *Fragments*: 'Black' (10YR 2/1)	Calcite ($CaCO_3$) Quartz low (SiO_2) Goethite (Fe(O)OH) Magnetite (Fe_3O_4) Kaolinite ($Al_2Si_2O_5(OH)_4$)
3	A) Very fine (lower) Very well sorted Occasional horizons of increased pebbles and sand	**Average**: 26 ± 12 g/cm^3 **Modal Freq.**: 52.38% 15 g/cm^3< x < 21 g/cm^3 (n = 21)	8% ± 1	Echinoderm spines and shell fragments dating to the Eocene in coarse horizons	*General*: 'Strong brown' (7.5YR 4/6) *Laminations: 'Yellow' (10YR 7/8)*	Goethite (Fe(O)OH) Magnetite (Fe_3O_4) Calcite ($CaCO_3$) Quartz low (SiO_2
4	A) Very fine (lower) Well sorted Occasional horizons of increased pebbles and sand	**Average**: 29 ± 22 g/cm^3 **Modal Freq.**: 81.25% 10 g/cm^3< x < 45 g/cm^3 (n = 64)	7 % ± 1	Echinoderm spines and shell fragments dating to the Eocene in coarse horizons	*General*: 'Very dark brown' (7.5YR 2.5/2) *Laminations*: 'Yellow' (10YR 7/8) 'Black' (10YR 2/1)	Birnessite ((Na0.3Ca0.1K0.1)(Mn)$_2$O$_4$) Jacobsite ($MnFe_2O_4$) Ramsdellite (MnO_2) Goethite (Fe(O)OH) Calcite ($CaCO_3$) Quartz low (SiO_2)
5	A) Very fine (lower) Very well sorted B) Large horizons with increased pebbles and sand	**Average**: 18 ± 28 g/cm^3 **Modal Freq.**: 61.76% < 10 g/cm^3 (n = 68)	8% ± 1	Echinoderm spines and shell fragments dating to the Eocene in coarse horizons	General: 'Dark reddish brown' (5YR 3/4) Laminations: 'Dark brown' (7.5YR 2.5/3) 'Brownish yellow' (10YR 6/8)	Goethite (FeO(OH)) Calcite ($CaCO_3$) Quartz low (SiO_2)
6	Coarse lower Very well sorted	**Average**: 1074 ± 59 g/cm^3	<1% ± 1	No visible fossils	General: 'White' (10YR 8/1)	Silica sand: likely Quartz low (SiO_2)

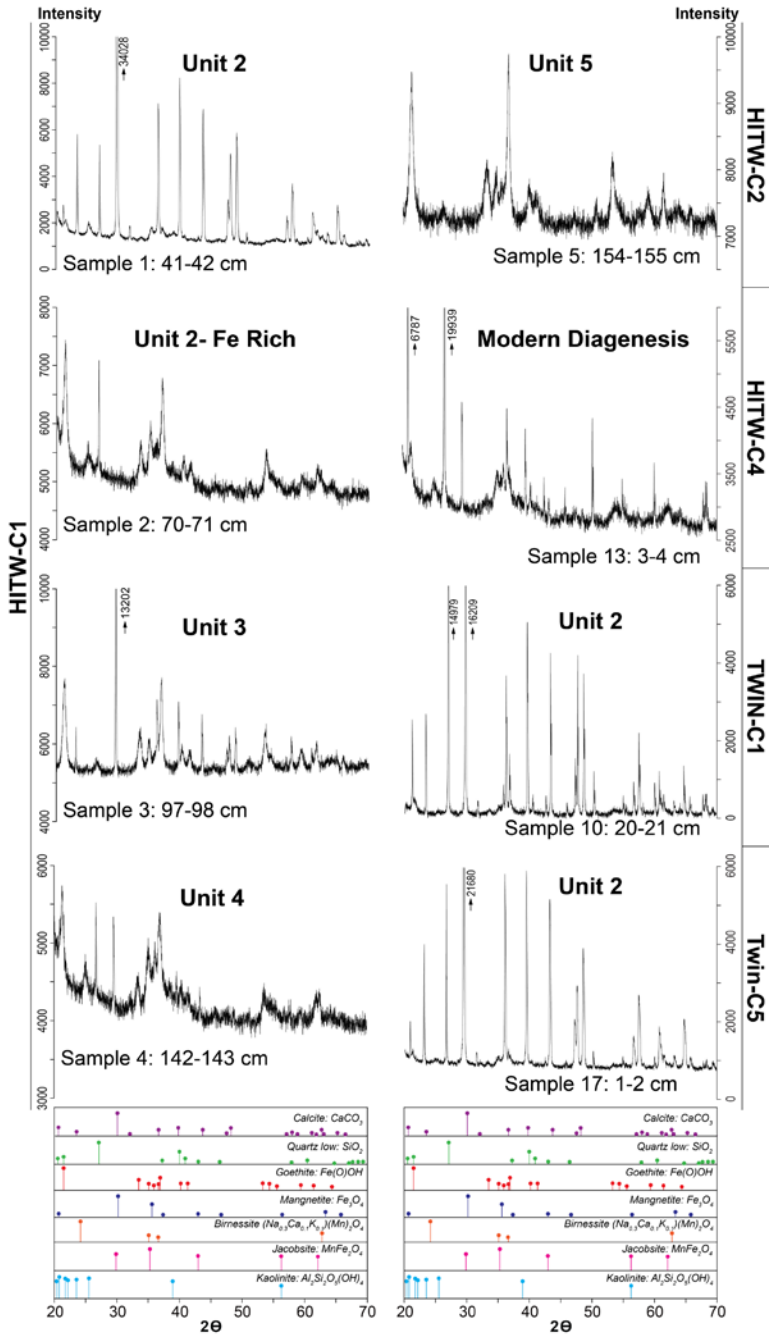

Figure 6: Selected diffractograms generated from XRD analysis of sediment samples from HITW Cave and Twin Cave.

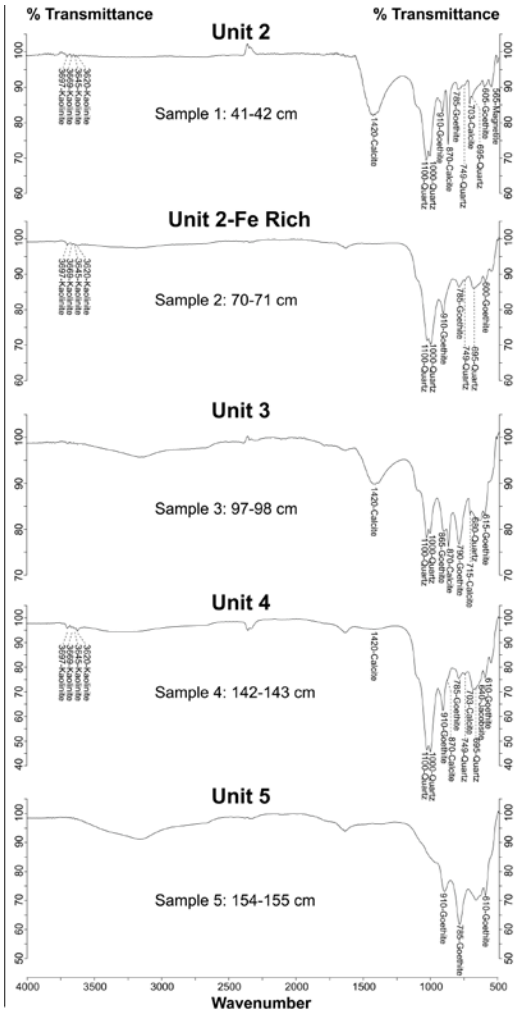

Figure 7: Spectrographs generated from FTIR analysis of sediment samples S1-S5 in HITW-C1

Age and correlations

Using the results of radiocarbon dating, it was determined that all of the cores taken from HITW Cave had a single unit of organic matter that was deposited as the uppermost most stratigraphic layer in these cores. Radiocarbon analysis of bulk organic matter sampled at 35-36 cm in HITW-C1 and 34 to 35 cm in HITW-C2 provided respective dates of 5630 ± 30 and 5530 ± 60 Calibrated Years Before Present (Cal yrs BP), marking the onset of Unit 1 deposition in HITW

Cave. Radiocarbon analysis of sediment sampled from 0 to 1 cm in HITW-C2 revealed that accumulation of Unit 1 sediments ceased at approximately 3550 ± 75 Cal yrs BP (Table 1). TWIN-C1 and C6 each have a small unit of bulk organic matter that appears as within the most recently deposited stratigraphic unit and an additional large pulse of organic matter that occurs as the second distinct stratigraphic unit in the core. Radiocarbon analysis of sediments sampled at 0 to 1 cm and 4.5 to 5.5 cm in TWIN-C1 produced respective dates of 5170 ± 130 and 3920 ± 50 Cal yrs BP, indicating that deposition of this organic matter occurred around the same period of time as the large accumulations of organic matter seen in HITW-C1 and HITW-C2 (Fig. 4). TWIN cores 1, 2, 3, and 4 all contained evidence of a large pulse of bulk organic matter located directly below the most recent stratigraphic unit that have more intact leaf-like bulk organic matter in a matrix of very fine grained organic matter. Radiocarbon analysis of bulk organic matter sampled from the bottom (66.5 to 67.5 cm) and the top (23 to 24 cm) of a bulk organic matter unit in TWIN-C1 resulted in respective dates of 13,930 ± 190 and 13950 ± 160 Cal yrs BP, implying that this 43.5 cm pulsed was deposited in a geologic instant. The stratigraphic location along with the leafy texture of the bulk organic matter units in TWIN-C2, TWIN-3, and TWIN-C4 indicates that each of these units are likely correlated to the same event driven pulse as shown by the correlation bars in Fig. 4. Twin-C5 is the only core that was collected in our coring survey of both HITW Cave and Twin Cave Unit 1 does not appear (Fig. 4), making it difficult to temporally correlate sediments in this core to other cores from this system.

Aside from bulk organic matter from Unit 1, there is no substantial organic matter content in any of the other lithofacies. The precise onset of sediment accumulations also remains unknown as no datable material was recovered from the base-level of either cave system. Furthermore, to the

lack of datable material in Units 2-6, the precise age of deposition remains unknown for these lithofacies and they cannot be correlated temporally. All stratigraphic-lithological correlations between Units 2-6 (Fig. 4) are based upon corresponding: Munsell color (Table 2), elemental composition (Fig. 4), mineralogy (Fig. 6, 7), texture (coarse sediment fraction) (Fig. 4), and organic matter composition (Fig. 4).

Water quality

Water quality data collected from HITW Cave and Twin Cave revealed that both caves currently exhibit homogenous freshwater hydrologic conditions (Fig. 8).

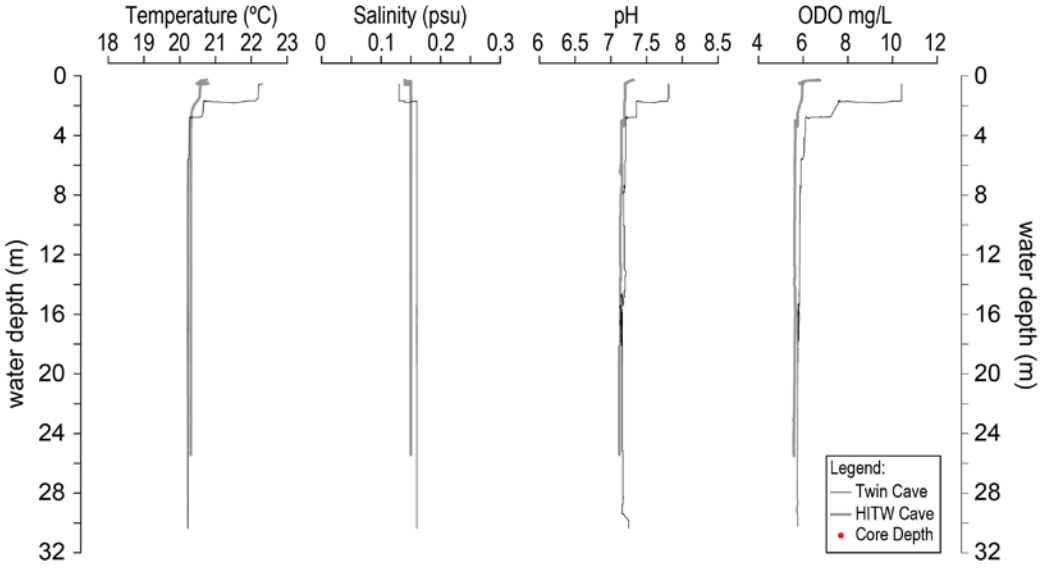

Figure 8: Profiles of water temperature (ºC), salinity (psu), pH, and ODO (mg/L) in HITW Cave and Twin Cave.

CHAPTER IV

DISCUSSION

Considering the textural variability, organic matter content, elemental and mineralogical composition, and relative timing of accumulation, the sediments recovered from HITW Cave and Twin Cave can be grouped into three broad categories of sedimentary style: *Iron and manganese oxides and oxyhydroxides* (Units 3, 4, 5, and often Unit 2A), *texturally-variable carbonate sedimentation* (Unit 2), and *gyttja* (Unit 1). It is likely that variations in sediment supply, aquifer hydrology, and regional and global climate and sea-level variability all played a role influencing long-term sedimentation in these caves.

Iron and manganese oxides and oxyhydroxides

The basal sediments recovered from HITW cave are dominated by metal oxides, most commonly iron and manganese oxides and oxyhydroxides (e.g., goethite (Fe(O)OH), birnessite ($(Na_{0.3}Ca_{0.1}K_{0.1})(Mn)_2O_4$), etc.) (Fig. 6, 7). Due to the lack of temporal constraint on their deposition, interpreting the environmental conditions or events responsible for their emplacement remains a challenge. The presence of iron oxide sediments has been recorded in multiple studies of cave sediments (Fornós et al., 2009; Onac et al., 2014; Onac et al., 2001; van Hengstum et al., 2011). To our knowledge, however, never before have iron and manganese oxide and oxyhydroxide deposits of this thickness been noted in phreatic caves. Accumulation of iron-rich Saharan dust has been previously suggested as a potential source of iron rich sediments in phreatic caves (Fornós et al., 2009), however this alone is not a large enough source to account for sheer volume of iron and manganese oxide and oxyhydroxide rich sediments in HITW Cave

and Twin Cave. An alternate hypothesis is that these sediments have an autochthonous origin, whereby long-term precipitation of iron and manganese oxides and oxyhydroxides resulting from upwelling of iron and manganese rich groundwater into well oxygenated, pH neutral cave water not only accounts for the volume of sediment but could also explain why these lithofacies exhibit varied, high-frequency laminations. By applying the basic principles of redox chemistry, it is possible to hypothesize what types of hydrologic conditions in HITW Cave, Twin Cave, and the Western Floridian aquifer may have existed in the past based on the speciation of precipitated iron and manganese oxides and oxyhydroxides.

Due to their redox sensitive behavior, iron and manganese oxides and oxyhydroxides are common minerals in sediments in a wide variety of aquatic sediments that can accumulate in either oxic or anoxic conditions (Bozau et al., 2008; Davison, 1993; Emerson, 1976; Emerson and Widmer, 1978; Jones and Bowser, 1978; Naeher et al., 2013; Van Breemen, 1988). The specific mineralogy of precipitated minerals has been shown to be dominated primarily by water oxidation levels and pH in both laboratory (Cornell and Giovanoli, 1987; Fischer and Schwertmann, 1975; Gotić et al., 2008; Lind et al., 1987; Onac et al., 2014; Onac et al., 2001; Onac et al., 1997; Schwertmann and Murad, 1983) and natural environments (Davison, 1993; Jones and Bowser, 1978; Naeher et al., 2013; Pham et al., 2006; Rose and Waite, 2003; Spiteri et al., 2006). In anoxic depositional settings, such as wetlands or stratified lakes, conditions in water often result from bacterial oxygen consumption during organic matter decomposition (Davison, 1993). In anoxic aquatic environments, iron (III) and manganese (III/IV) ions are readily reduced to thermodynamically favorable Fe (II) and Mn (II) ions that are either transported upwards in the water column or incorporated into the lattice of clay minerals (De

Vitre and Davison, 1993). Inversely, iron (II) and manganese (II) are thermodynamically unstable under oxidized, pH neutral water conditions, and have been shown to readily oxidize into insoluble iron (III) and manganese (III/IV) oxides and oxyhydroxides (De Vitre and Davison, 1993; Martin, 2005). Some of the more common iron (III) and manganese (III/IV) oxides and oxyhydroxides that form in natural aquatic environments under oxic conditions include: goethite (Fe(O)OH), magnetite (Fe_3O_4), birnessite ($(Na_{0.3}Ca_{0.1}K_{0.1})(Mn)_2O_4$), manganosite (MnO), and manganite (γ-Mn(O)OH) (Davison, 1993; Lind et al., 1987).

The results of elemental and mineralogical analysis indicate that iron oxides and oxyhydroxides, particularly goethite (Table 1, Fig. 7, 8), dominate the sedimentation throughout sedimentary Units 3, 4, and 5 as well as fine grained portions of Unit 2A. Though the precise mineralogical structure naturally precipitated manganese oxides and oxyhyroxides can be difficult to determine due to their extreme microcrystalinity (Davison, 1993; Lind et al., 1987), it appears that the manganese oxide minerals birnessite ($(Na_{0.3}Ca_{0.1}K_{0.1})(Mn)_2O_4$) and jacobsite ($MnFe_2O_4$) (Table 1, Fig. 6, 7) are present in small quantities throughout Units 2, 3, 5 and are found in large quantities in the manganese rich Unit 4 based on the intensity of the correlated peaks in the XRD diffractograms (Fig. 6) and the overall increase in elemental manganese according to the results of XRF analysis (Fig. 4). Based on iron and manganese redox behavior studies conducted in both laboratory (Gotić et al., 2008; Martin, 2005; Schwertmann and Murad, 1983) and natural conditions (Charette and Sholkovitz, 2002; Davison, 1993; Pham et al., 2006; Rose and Waite, 2003; Spiteri et al., 2006), the minerals observed throughout Units 2A, 3, 4, and 5 are likely to have precipitated in well oxidized water with a pH range of 6 to 8. The increase in manganese oxides and oxyhydroxides noted in Unit 4 is most likely caused by an increase in the dissolved

oxygen levels or the pH of the cave water (Cornell and Giovanoli, 1987; Davison, 1993; Naeher et al., 2013). Fe (II) has a higher oxidation state than Mn (II); therefore, iron oxides and oxyhydroxides precipitate more rapidly than their manganese counterparts, thus requiring higher levels of dissolved oxygen to oxidize high levels of manganese (Davison, 1993; Naeher et al., 2013).

As discussed later in this study, both HITW Cave and Twin Cave appear to have experienced rapid pulses of bulk detrital organic matter at 5630 ± 30 to 3550 ± 75 Cal yrs BP and 13,950 ± 160 to 13,930 ± 190 Cal yrs BP. During these pulses, sediments have very little to no elemental iron or manganese and no visual accumulations of iron or manganese oxides or oxyhydroxides based on color. In natural waters, organic ligands such as oxalate and humic acid have been shown to increase the dissolution rates of iron and manganese oxides (Martin, 2005; Stone, 1997). The pulses of organic matter and the subsequent increase in organic ligands could explain why Unit 1 sediments lack the iron and manganese oxide and oxyhydroxide minerals present throughout the other lithofacies.

Modern hydrogeochemistry in HITW Cave and Twin (Fig. 8) is indicative of homogenized freshwater that is pH neutral and well oxidized. HITW Cave has an average pH of 7.157 ± 0.038 and an average ODO of 5.689 mg/L and Twin Cave nearly mirrors the water profile of HITW cave with a mean pH of 7.178 ± 0.151 and an ODO of 5.913 ± 0.543 mg/L. In each of the cores collected from HITW Cave, a 1 to 3 cm accumulation of “yellowish red” (5YR 4/6) sediment occurs at the sediment water interface. XRD analysis of mineralogy of this unit indicates that it is rich in goethite, quartz, and calcite similarly to iron rich portions of Unit 2A (Fig. 6). Based on

the principles of redox chemistry as well as the mineralogy of sediments through the cores, this unit is most likely a modern redox boundary dominated by goethite precipitation. If this is the case, it is possible that modern hydrologic conditions in these systems are similar to those that occurred during the period when iron and manganese oxide and oxyhydroxide rich lithofacies such as units 3, 4 and 5 were deposited. As a result of the absence of datable material in or around Units 2-A, 3, 4, and 5 (Fig. 4) it cannot be said precisely when these units were deposited which limits the usefulness of these sediments as a paleoclimate archive.

Hydrodynamic variability and the deposition of coarse sediments

Another primary sedimentary style in these phreatic caves is the *texturally-variable carbonate sedimentation* (Unit 2) with variable iron and manganese content. Intermittent horizons of coarse sediments (> 63 μm) appear at varying frequencies throughout all lithofacies in HITW Cave and Twin Cave. These horizons are rare in Unit 1, 2A, 3, 4, and 5 and can generally be attributed to the increased deposition of quartz sand or marine echinoid fossils (Fig. 4, 5). It is likely that these fossils were eroded out of the surrounding Ocala limestone as this formation is described as being rich in Eocene echinoid, mollusks, bryozoan, and foraminifera fossils (Cooke, 1945; McKinney and Zachos, 1986; Schmidt, 1984; Schmidt, 1988). Unit 2B and C as well as Unit 6 are the only lithofacies that show large accumulations of coarse grained sediments (Fig. 4; Table 2). By applying the basic principles of sedimentary erosion, transport as deposition as detailed by the Hjulström curve, it is likely that Units 2-B, 2-C, and 6 record periods of increased hydrologic flow into or within the cave systems (Quade et al., 1995). The increase in flow could be related to a number of factors such as increased precipitation or sea-level rise. Another factor that could be influencing the higher levels of deposition of fossils and coarse grained particulates in the

sedimentary record is that a rise in the pH of the cave water could result in partial dissolution of the surrounding Ocala limestone. This partial dissolution would target the calcium carbonate lithification, releasing partially silicified fossils and particulates that are then deposited on the floor of the cave in the sedimentary record.

The accumulation *texturally-variable carbonate sediments* (Unit 2) likely represents a period of regional subterranean variability in hydrographic velocity change, but the timing and sedimentary budget remains challenging to resolve. The richness of Eocene-aged marine fossils within the fine grained calcium carbonate matrix indicates that this sediment is autochonous and could indicate a period of cave expansion. Answering the questions of where these *texturally-variable carbonate sediments* (Unit 2) came from and when they were deposited could have important implications towards further understanding the mechanisms of inland phreatic cave speleogenesis and thus merit further study.

Pulsed supply of organic matter during the last 15,000 years

In order to interpret the stratigraphy of sediment in inland phreatic caves, it is important to understand the processes of deposition, the source of sediment, therefore important to understand the concepts behind of facies analysis. Primary productivity in phreatic caves is generally very low (Iliffe et al., 1984; Pohlman et al., 1997); therefore, autochthonous organic matter sources are insignificant in relation to the overall sedimentary budget of most phreatic cave systems. As such, input of allochthonous organic matter plays a major role in environmental development (Fichez, 1990; Franz et al., 1994; Gibert et al., 1994; Opsahl and Chanton, 2006; Opsahl et al., 2005; Panno et al., 2004; Pohlman et al., 1997) and the presence of organic matter in

sedimentary accumulations can be utilized as a tool in understanding paleohydrologic change such as groundwater or surface flow reversals (Fornós et al., 2009; Opsahl et al., 2005) and sea-level rise (van Hengstum and Scott, 2012; van Hengstum et al., 2011).

Based on the established principles of organic matter source and abundance in phreatic cave systems outlined above, it is very likely that the organic matter in Unit 1 was brought into HITW Cave and Twin Cave during periods in which groundwater flow reversed and caused these systems to function as siphons. As discussed in the "Correlations and Age" section of the results, radiocarbon dating of bulk organic matter taken from the top and bottom of Unit 1 lithofacies in TWIN-C1, HITW-C1, and HITW-C2 reveal that of deposition of these units occurred rapidly in pulsed supply. Using the results of radiocarbon dating analysis as well as qualitative sediment textural characteristics, two temporally and stratigraphically distinct pulses, Organic Matter Pulse-1 (OMP-1) and Organic Matter Pulse-2 (OMP-2), were identified in these systems (Fig. 9).

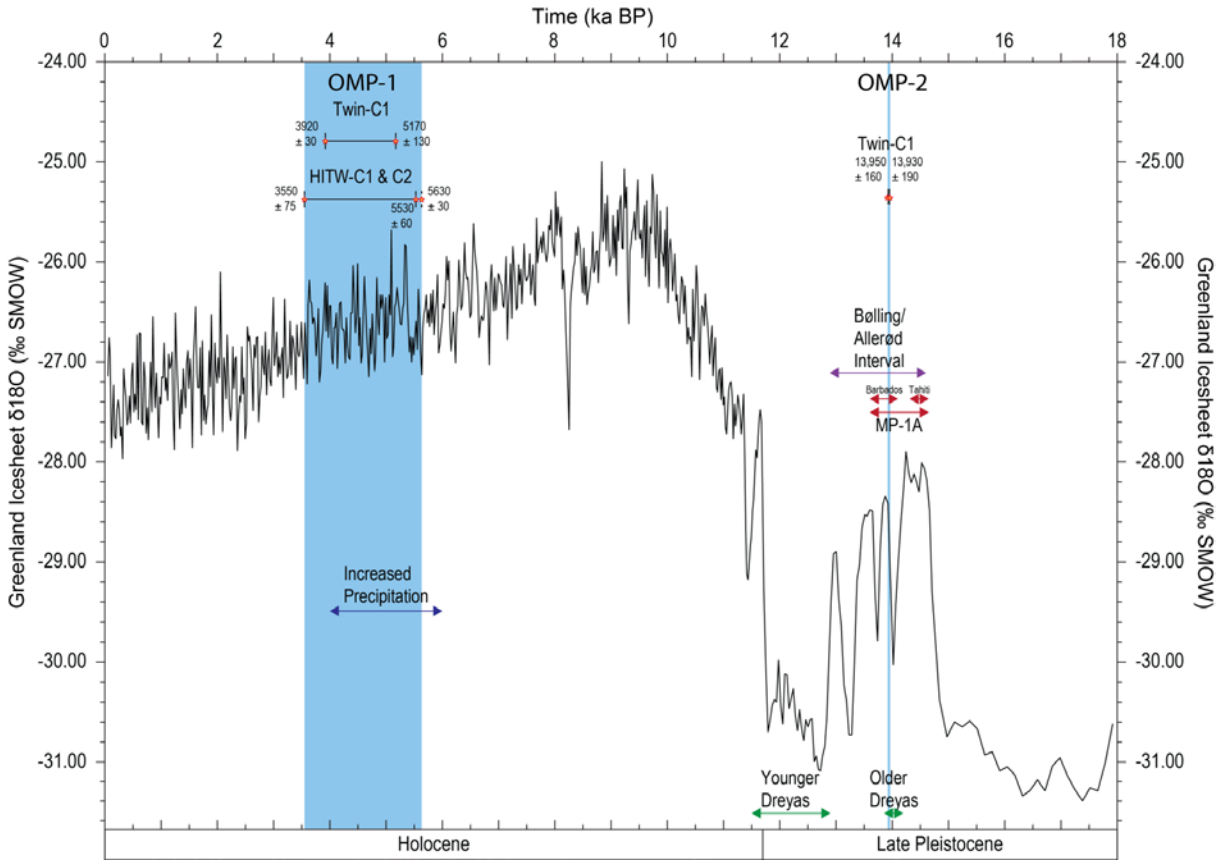

Figure 9: $\delta^{18}O$ isotopic curve from Renland Ice Cores in Eastern Greenland (Vinther et al., 2008). The depositional age ranges of OMP-1 and OMP-2 based on radiocarbon dates from HITW-C1 and C2 and TWIN-C1 (yellow and red stars) are indicated in this figure. Important climatic shifts such as the initiation of the Bølling/Allerød Interstadial and Meltwater Pulse 1-A at ~14,000 Cal yrs BP and an increase in precipitation at ~5000 Cal yrs BP that marks the onset of modern climatic conditions in the Southeastern United States are also indicated in the lower portion of the figure.

Organic Matter Pulse-1 (OMP-1)

OMP-1 occurred from 13,950 ± 160 to 13,930 ± 190 Cal yrs BP based on the maximum range of radiocarbon dates sampled from the top and bottom of Unit 1B in TWIN-C1 (Table 1; Fig. 9). Though no other radiocarbon dates from Unit 1B sediments were obtained, it was decided that the Unit 1 lithofacies that occurred in TWIN-C2, C4, and C6 were deposited in correlation with OMP-1 based on the more intact leafy detrital organic matter that was observed in Unit 1B sediments in Twin-C1. As such, these units were likely deposited in the same 13,950 ± 160 to

13,930 ± 190 Cal yr BP timeframe as Unit 1B sediments in TWIN-C1. The oldest radiocarbon date in Unit 1B (13,950 ± 160 Cal yrs BP) is attributed to bulk organic matter sampled from 23 to 24 cm at the bottom of Unit 1B in TWIN-C1. The most recent date obtained from sediment in Unit 1B (13,930 ± 190 Cal yrs BP) comes from bulk organic matter sampled from 66.5 to 67.5 cm at the top of Unit 1B in TWIN-C1.

The late Pleistocene deposition of Unit 1B organic matter at ~14,000 yrs BP correlates with dynamic changes in both regional and global climate and sea level that seem to mark the transition from the Wisconsin Glaciation to the onset of the Holocene. The deposition of OMP-1 appears to have occurred during the Bølling/ Allerød Interstadial; a period in which global climate rapidly shifted from a state of glaciation towards warmer, moist climate conditions from ~14,700 yrs BP to the onset of the Younger Dreyas at ~12,700 yrs BP (Bard et al., 2010; Deschamps et al., 2012). Based on pollen reconstructions from Camel Lake (~60 km southwest of Merritts Mill Pond) (Watts et al., 1992) and Sheelar Lake (Watts, 1980), Northwestern Florida was dominated by mesic, deciduous forests through the Bølling/ Allerød Interstadial which would indicate that the precipitation was low during this period. Furthermore, the pollen reconstruction from Camel Lake recorded a peak in spruce pollen from 14,330 ± 275 yrs BP to 12,610 ± 135 yrs BP that would indicate that temperatures in this region (Watts et al., 1992). This indicates that regional climate in Northwestern Florida during the Bølling/ Allerød Interstadial was actually much colder than it is in modern conditions (Watts et al., 1992), behaving paradoxically to the global trend towards warmer, wetter environments during this period. The regional cooling of Northwestern Florida during the Bølling/ Allerød Interstadial is most likely related to cooling of the Gulf of Mexico caused by Mississippi River discharge of

Meltwater Pulse-1A (MWP-1A) from the Laurentide Ice Sheet between 14,650 yrs BP (Deschamps et al., 2012)and 13,600 yrs BP (Bard et al., 1990; Fairbanks, 1989). In addition to raising global sea surface temperatures, MWP-1A also rapidly changed relative sea level by as little as 0.66 ± 0.07 m (Wickert et al., 2013) or as much as 17 ± 5 m (Deschamps et al., 2012). This rise in sea level could have had a significant effect on the level of the water table in Northwestern Florida, perhaps even facilitating short-lived formation of surface streams and pools. Such changes in surface and groundwater hydrology could have caused the deposition of OMP-1.

Based on the error in the calibrated radiocarbon dates from the bulk organic matter sampled in TWIN-C1, it could be argued that this 44.5 cm accumulation of organic matter was deposited over a 100 to 200 year period in response to a continuous change in the regional hydrography. However, the temporal anomaly in which the more recent radiocarbon date was obtained from sediment 44.5 cm deeper within the sedimentary record indicates that an exterior accumulation of sediment was rapidly eroded and transported in a single event that caused the mixing of old and new organic deposits. This hypothesis that Unit 1B was deposited in a single pulse event (OMP-1) is further supported by the tight temporal constraint on the radiocarbon dates, the homogenous texture of the sediment, and the rapid, dramatic change in both global and regional climate, sea level, and hydrology.

Organic Matter Pulse-2 (OMP-2)

OMP-2 was deposited between 5630 ± 30 to 3550 ± 75 Cal yrs BP based on the maximum range of radiocarbon dates sampled from the top and bottom of Unit 1A in TWIN-C1, HITW-C1, and

HITW-C2 (Table 1; Fig. 9). The depositional period of Unit 1A in every core from HITW Cave and Twin Cave is likely to fall somewhere within this established age range. The timing of OMP-2 closely correlates to the rise of relative sea level to near modern levels as well as the establishment of the modern climatic regime in the Southeastern United States between 5700 and 4000 yrs BP (Clausen et al., 1979; Grimm et al., 1993; Watts et al., 1992; Watts and Hansen, 1994; Winkler et al., 2001; Zarikian et al., 2005). Warming atmospheric temperatures and the rise of the sea surface began to promote high levels of precipitation in this region at ~5000 yrs BP (Delcourt, 1980; Zarikian et al., 2005) that subsequently established the modern pine forests that dominate the vegetation in this region (Delcourt, 1980; Grimm et al., 1993; Grimm et al., 2006; Watts et al., 1992; Watts, 1969). The rise of sea level along with increased levels of precipitation between ~8000 and ~5000 yrs BP raised the regional water tables which ultimately caused the flooding of many modern surface hydrological features such as lakes (Watts and Hansen, 1988; Watts and Hansen, 1994; Watts and Stuiver, 1980), ponds (Delcourt, 1980; Zarikian et al., 2005), and streams (Cohen et al., 1984; Gulley et al., 2014; Gulley et al., 2012) that were previously dry. It is therefore entirely possible that Merritts Mill Pond was a dry surface basin until ~5000 Cal yrs BP and that flooding of this feature eroded surface sediment accumulations and washed them into HITW Cave and Twin Cave where they were deposited.

If OMP-2 was deposited in a single pulse event, it would explain the temporal anomaly of Unit 1A in TWIN-C1 in which sediment from 0 to 1 cm was dated at 5170 ± 130 Cal yrs BP while sediment from 23 to 24 cm in this same core was placed at of 3920 ± 50 Cal yrs BP, thus violating the Law of Superposition. If an exterior accumulation of organic matter rich sediments was transported into the cave and deposited in single, rapid pulse event (such as OMP-1 which is

hypothesized to have deposited Unit 1B) the original stratigraphic arrangement would likely be reworked dramatically, potentially resulting in temporal anomaly such as the one observed.

It is possible that Unit 1A was deposited continuously from ~5600 Cal yrs BP to ~3500 yr as runoff from consistently high levels of precipitation transported modern organic deposits into the cave systems until little or no sediment remained in Merritts Mill Pond as it exists in its modern state. This hypothesis works well for Unit 1A in HITW Cave as the oldest dated sediments are deposited below the younger dated sediments at the top of the core. However, this model fails to explain the temporal anomaly that occurs in dated sediments from Unit 1A in TWIN-C1 and is therefore less likely to have occurred than the hypothesis that Unit 1A sediments were deposited in a single pulse, OMP-2.

Though no radiocarbon dates were obtained from Unit 1 sediments in TWIN-C3, the presence of modern freshwater gastropods along with the fact that this core was taken in the location most proximal to the cave entrance of any of the cores in this survey indicates that that modern sedimentation is being recorded in this core. It is very likely that the onset of organic matter accumulation in TWIN-C3 correlates to the onset of OMP-2; however, Unit 1A is far larger in this core than it is in any of the other cores taken from Twin Cave. The length of Unit 1A in TWIN-C3, the short distance from the cave entrance, and the presence of freshwater gastropod shells in the stratigraphy all indicate that this core includes modern sediments deposited during siphon phases in Twin Cave.

Though many differences exist in the climatic regimes in which OMP-1 and OMP-2 were deposited, both pulses occurred in a time of rapid sea level rise that raised the regional water table and allowed surface streams and pools to form. OMP-1 and OMP-2 likely mark significant flow reversals within these cave systems that occurred when surface flooding events caused river stage to increase faster than hydrologic head of the Floridian Aquifer (Gulley et al., 2011), ultimately resulting in the deposition of allochthonous *Organic Matter Pulses* (Unit 1).

Groundwater levels and flooding sequence

As discussed in the "Study Site" section of this paper, sea level fluctuations and precipitation are believed to have affected regional groundwater hydrography such that inland karst formations have oscillated between vadose and phreatic conditions throughout geologic time (Florea et al., 2007; Gulley et al., 2012; LeGrand and Stringfield, 1966). Caves in the same region as HITW Cave and Twin Cave are believed to have formed during vadose conditions in an eogenetic karst aquifer as a result of CO_2 enrichment of lower water tables that were subsequently flooded by the Floridian aquifer in response to sea level rise (Gulley et al., 2012). Assuming that the Northwestern Floridian aquifer exhibits the synchronous rise in response to deglacial sea level rise observed in the northern central Florida (Gulley et al., 2014; Gulley et al., 2011; Gulley et al., 2012) and peninsular Florida (Florea et al., 2007), it is hypothesized that the onset of sedimentation occurred around the timeframe in which sea level was at a low stand during the last glacial maximum ~20,000 yrs BP. By compiling the discontinuous sedimentary records recovered from HITW Cave and Twin Cave, a model for the potential sedimentary response to late quaternary deglaciation and subsequent sea level rise is proposed in detail in the following paragraph.

The earliest sedimentation period sampled is hypothesized to be characterized by *Iron and manganese oxides and oxyhydroxides* (Units 3, 4, 5) that precipitated in well-oxygenated aquatic cave conditions. Sometime between ~20,000 yrs BP and ~14,000 yrs BP, sedimentation switched to deposition of *texturally-variable carbonate sediments* (Unit 2). This type of sedimentation is hypothesized to be related to periods of cave expansion in which a shift in groundwater hydrology that may include increased flow and a change in hydrogeochemistry related to CO_2 gas diffusion into the water table (Gulley et al., 2012). At ~14,000 yrs BP, rapid sea-level rise related to the Bølling/Allerød Interstadial and MWP-1A raised the regional water table. Based on the results of this study, it is hypothesized that the rise in the regional water table was significant enough to have caused a rapid, short-lived appearance of surface streams in Northwestern Florida that flooded into a surface opening of Twin Cave and deposited OMP-2 *organic matter sediments* (Unit 1B) was on top the *texturally-variable carbonate sediments* (Unit 2). There is no evidence of Unit 1B organic matter sediments related to OMP-2 in any of the cores recovered from of HITW Cave which indicates that the surface entrance to this cave had not yet formed or that recovered sedimentary records did not extend deep enough into sediment accumulations in this cave. However, the small size of the semicircular entrance to HITW Cave in its current state (~ 0.75 m diameter) indicates that perhaps the entrance to this cave is a relatively modern feature, forming sometime after OMP-1. After the deposition of OMP-1 *gyttja* (Unit 1B), sedimentation appears to shift back to deposition of *texturally-variable carbonate sediments* (Unit 2), indicating further cave expansion until the deposition of OMP-2 *gyttja* (Unit 1A) at ~5600 Cal yrs BP. Holocene sea-level rise steadily raised the Floridian water table, resulting in the formation of surface water features as early at ~8000 yrs BP (Watts and Hansen, 1988). The onset of OMP-2 deposition correlates to the time in which sea level had risen to ~6 m below

modern levels (Fairbanks, 1989) and the onset of modern Floridian climatic conditions. These factors together likely caused massive flooding of surface hydrologic features that exceeded the hydrologic head of the aquifer and caused a flow reversal in HITW Cave and Twin Cave during which OMP-2 *gyttja* (Unit 1A) accumulated. The accumulation of OMP- *gyttja* (Unit 1A) also indicates that the entrance to HITW Cave formed at some point before ~6300 yrs BP but after the deposition of OMP-1 *gyttja* (Unit 1B) ~14,000 yrs BP. The appearance of iron and manganese oxides and oxyhydroxides in the upper 10 cm of HITW-C3, C4, and C5 and well as TWIN-C4, C5, and C6 indicates that a modern redox boundary exists in these caves and is resulting in diagenesis of these sediments.

Conclusions

This study provides the first assessment of the usefulness of sediments from inland phreatic caves as archives of paleohydrologic response to climatic variability. Six distinct lithofacies were identified in sediment cores collected in HITW Cave and Twin Cave in Marianna, FL. These lithofacies can be grouped further into three broad categories of sedimentary style: *iron and manganese oxides and oxyhydroxides* (Units 3, 4, 5, and often Unit 2A), *texturally-variable carbonate sedimentation* (Unit 2), and *Organic Matter Pulses (OMP)* (Unit 1). Each of these sedimentary styles can be associated with distinct hydrologic conditions that correlate with environmental change forced as a result of sea level rise in response to the termination of the Last Glacial Maximum ~20,000 yrs BP. *Iron and manganese oxides and oxyhydroxide* (Units 3, 4, 5, and often Unit 2A) sediments likely represent base level sedimentation in these systems, precipitating in redox conditions during a partially flooded sump phase of these cave systems. *Texturally-variable carbonate sedimentation* (Unit 2) that occurs twice in the hypothesized

sedimentary sequence (Fig. 10) is likely related to cave expansion related to variation in hydrologic conditions. *gyttja (OMP)* (Unit 1) contain the only sediment that is suitable for radiocarbon dating and is therefore the only sedimentary group that can be precisely temporally constrained. *gyttja (OMP)* (Unit 1) appear to deposited in relation to the reversal of cave hydrologic flow caused by the formation and subsequent flooding of surface water features in response rise in the regional water table forced concurrently by sea level rise and increased precipitation.

Unfortunately, the lack of datable material throughout all lithofacies other than *Organic Matter Pulses (OMP)* (Unit 1) makes it challenging to place precise temporal constraint on the depositional period of the *iron and manganese oxides and oxyhydroxides* (Units 3, 4, 5, and often Unit 2A) and the *texturally-variable carbonate sediments* (Unit 2). The inability to temporally constrain the majority of the sediments in these caves combined with the highly discontinuous sedimentary record that is caused by sedimentary bypass in relation to complex geometry of HITW Cave and especially Twin Cave severely hampers the usefulness of these sediments these systems as long term indicators of paleohydrologic variability. However, the results of this study indicate that sediments in inland phreatic caves do show a corollary response to hydrologic variability of the aquifer during times of dramatic environmental change and that further study of these sediments could begin to fill in gaps that currently exist in the sedimentary of late quaternary groundwater variability in Florida.

REFERENCES

Alverez Zarikian, C.A., Swart, P.K., Gifford, J.A., Blackwelder, P.L., 2005. Holocene paleohydrology of Little Salt Spring, Florida, based on ostracod assemblages and stable isotopes. Palaeogeography, Palaeoclimatology, Palaeoecology 225, 134-156.

Bard, E., Hamelin, B., Delanghe-Sabatier, D., 2010. Deglacial meltwater pulse 1B and Younger Dryas sea levels revisted with boreholes at Tahiti. Science 327, 1235-1237.

Bard, E., Hamelin, B., Fairbanks, R.G., 1990. U-Th ages obtained by mass spectrometry in corals from Barbados: sea level during the past 130, 000 years. Nature 346, 456-458.

Bosch, R.F., White, B., 2007. Lithofacies and transport of clastic sediments in karstic aquifers, in: Sasowsky, I.D., Mylroie, J. (Eds.), Studies of Cave Sediments. Kluwer Academic Publishers, pp. 1-22.

Bozau, E., Göttlicher, J., Stärk, H.-J., 2008. Rare earth element fractionation during the precipitation and crystallisation of hydrous ferric oxides from anoxic lake water. Applied Geochemistry 23, 3473-3486.

Brandon, C., Woodruff, J.D., Lane, P., Donnelly, J.P., 2013. Constraining flooding conditions for prehistoric hurricanes from resultant deposits preserved in Florida sinkholes. Geochemistry Geophysics Geosystems 14, 2993-3008.

Brown, A., Reinhardt, E.G., van Hengstum, P.J., Pilarczyk, J.E., 2013. A coastal Yucatan sinkhole records intense hurricane events. Marine Geology, submitted.

Bull, P.A., 1981. Some fine-grained sedimentation phenomena in caves. Earth Surface Processes and Landforms 6, 11-22.

Charette, M.A., Sholkovitz, E.R., 2002. Oxidative precipitation of groundwater-derived ferrous iron in the subterranean estuary of a coastal bay. Geophysical Research Letters 29, 85-81-85-84.

Clausen, C.J., Cohen, A.D., Emiliani, C., Holman, J.A., Stipp, J.J., 1979. Little Salt Spring, Florida: a unique underwater site. Science 203, 609-614.

Cohen, A.D., Spackman, W., Dolsen, P., 1984. Occurrence and distribution of sulfur in peat-forming environments of southern Florida. International Journal of Coal Geology 4, 73-96.

Cooke, C.W., 1939. Scenery of Florida interpreted by a geologist. Pub. for the state Geological survey.

Cooke, C.W., 1945. Geology of Florida. The Florida Geological survey.

Cornell, R., Giovanoli, R., 1987. Effect of manganese on the transformation of ferrihydrite into goethite and jacobsite in alkaline media. Clays and Clay Minerals 35, 11-20.

Davison, W., 1993. Iron and manganese in lakes. Earth-Science Reviews 34, 119-163.

De Vitre, R., Davison, W., 1993. Manganese particles in freshwater. Environmental particles 2, 317-352.

Delcourt, P.A., 1980. Goshen Springs: late Quaternary vegetation record for southern Alabama. Ecology, 371-386.

Denomee, K.C., Bentley, S.J., Droxler, A.W., 2014. Climatic control on hurricane patterns: a 1200-y near-annual record from Lighthouse Reef, Belize. Scientific Reports 4, 7.

Deschamps, P., Durand, N., Bard, E., Hamelin, B., Camoin, G., Thomas, A.L., Henderson, G.M., Okuna, J., Yokoyama, Y., 2012. Ice-sheet collapse and sea-level rise at the Bølling warming 14,600 years ago. Nature 483, 559-564.

Dodson, J., 2013. FINAL REPORT Nutrient TMDL for Jackson Blue Spring and Merritts Mill Pond (WBIDs 180Z and 180A). Florida Department of Environmental Protection, Division of Environmental Assessment and Restoration, Bureau of Watershed Restoration, Northwest District-Apalachicola-Chipola Basin, Tallahassee.

Emerson, S., 1976. Early diagenesis in anaerobic lake sediments: chemical equilibria in interstitial waters. Geochimica et Cosmochimica Acta 40, 925-934.

Emerson, S., Widmer, G., 1978. Early diagenesis in anaerobic lake sediments—II. Thermodynamic and kinetic factors controlling the formation of iron phosphate. Geochimica et Cosmochimica Acta 42, 1307-1316.

Fairbanks, R.G., 1989. A 17,000-year glacio-eustatic sea level record: influence of glacial melting rates on the Younger Dryas even and deep-ocean circulation. Nature 342, 637-642.

Fichez, R., 1990. Decrease in allochthonous organic inputs in dark submarine caves, connection with lowering in benthic community richness. Hydrobiologia 207, 61-69.

Fischer, W., Schwertmann, U., 1975. The formation of hematite from amorphous iron (III) hydroxide. Clays and Clay Minerals 23, 33-37.

Florea, L.J., Vacher, H.L., Donahue, B., Naar, D., 2007. Quaternary cave levels in peninsular Florida. Quaternary Science Reviews 26, 1344-1361.

Ford, D., Williams, P., 1989. Karst Geomorphology and Hydrology. Unwin Hyman, London.

Fornós, J.J., Ginés, J., Gràcia, F., 2009. Present-day sedimentary facies in the coastal karst caves of Mallorca island (western Mediterranean). Journal of Cave and Karst Studies 71, 86-99.
Franz, R., Bauer, J., Morris, T., 1994. Review of biologically significant caves and their faunas in Florida and South Georgia. Brimleyana, 1-109.

Gabriel, J.J., 2009. Late Holocene (3500 yBP) salinity changes and their climatic implications as recorded in an anchialine cave system, Ox Bel Ha, Yucatan, Mexico. McMaster University, p. 95.

Gabriel, J.J., Reinhardt, E.G., Peros, M.C., Davidson, D.E., van Hengstum, P.J., Beddows, P.A., 2009. Palaeoenvironmental evolution of Cenote Aktun Ha (Carwash) on the Yucatan Peninsula, Mexico and its response to Holocene sea-level rise. Journal of Paleolimnology 42, 199-213.

Gibert, J., Danielopol, D., Stanford, J.A., 1994. Groundwater ecology. Academic Press.

Gotić, M., Musić, S., Popović, S., Sekovanić, L., 2008. Investigation of factors influencing the precipitation of iron oxides from Fe (II) containing solutions. Croatica Chemica Acta 81, 569-578.

Grimm, E.C., Jacobson, G.L., Watts, W.A., Hansen, B.C.S., Maasch, K.A., 1993. A 50,000-year record of climate oscillations from Florida and its temporal correlation with the Heinrich events. Science 261, 198-200.

Grimm, E.C., Watts, W.A., Jacobson Jr, G.L., Hansen, B., Almquist, H.R., Dieffenbacher-Krall, A.C., 2006. Evidence for warm wet Heinrich events in Florida. Quaternary Science Reviews 25, 2197-2211.

Guilcher, A., 1988. Coral Reef Geomorphology. Wiley.

Gulley, J., Martin, J., Spellman, P., Moore, P., Screaton, E., 2014. Influence of partial confinement and Holocene river formation on groundwater flow and dissolution in the Florida carbonate platform. Hydrological Processes 28, 705-717.

Gulley, J., Martin, J.B., Screaton, E.J., Moore, P.J., 2011. River reversals into karst springs: A model for cave enlargement in eogenetic karst aquifers. Geological Society of America Bulletin 123, 457-467.

Gulley, J.D., Martin, J.B., Moore, P.J., Murphy, J., 2012. Formation of phreatic caves in an eogenetic karst aquifer by CO2 enrichment at lower water tables and subsequent flooding by sea level rise. Earth Surface Processes and Landforms 38, 1210-1224.

Hansen, B.C., 1990. ENVIRONMENTS OF FLORIDA IN THE LATE WISCONSIN AND HOLOCENE. Wet Site Archaeology, 307.

Heiri, O., Lotter, A.F., Lemcke, G., 2001. Loss on ignition as a method for estimating organic and carbonate content in sediments: reproducibility and comparability of results. Journal of Paleolimnology 25, 101-110.

Iliffe, T.M., Jickells, T.D., Brewer, M.S., 1984. Organic pollution of an inland marine cave from Bermuda. Marine Environmental Research 12, 173-189.

Jones, B.F., Bowser, C.J., 1978. The mineralogy and related chemistry of lake sediments, Lakes. Springer, pp. 179-235.

Kitamura, A., Yamamoto, N., Kase, T., Ohashi, S., Hiramoto, M., Fukusawa, H., Watanabe, T., Irino, T., Kojitani, H., Shimamura, M., Kawakami, I., 2007. Potential of submarine-cave sediments and oxygen isotope composition of cavernicolous micro-bivalve as a late Holocene paleoenvironmental record. Global Planetary Change 55, 301-316.

Kovacs, S.E., van Hengstum, P.J., Reinhardt, E.G., Donnelly, J.P., Albury, N.A., 2013. The late Holocene flooding history of Runway Sinkhole: a partially flooded coastal karst basin in the northern Bahamas. Quaternary International 317, 118-132.

Kyrle, G., 1923. Grundriß der theoretischen Speläologie. na.

Lane, P., Donnelly, J.P., Woodruff, J.D., Hawkes, A.D., 2011. A decadally-resolved paleohurricane record archived in the late Holocene sediments of a Florida sinkhole. Marine Geology 287, 14-30.

Larsen, E., Mangerud, J., 1989. Marine caves: on-off signals for glaciations. Quaternary International 3/4, 13-19.

LeGrand, H.E., Stringfield, V., 1966. Development of permeability and storage in the Tertiary limestones of the Southeastern States, USA. Hydrological Sciences Journal 11, 61-73.

Lind, C., Hem, J., Roberson, C., 1987. Reaction products of manganese-bearing waters. Chemical Quality of Water and the Hydrological Cycle, 273-301.

Martin, S.T., 2005. Precipitation and dissolution of iron and manganese oxides. Environmental Catalysis, 61-81.

McKinney, M.L., Zachos, L.G., 1986. Echinoids in biostratigraphy and paleoenvironmental reconstruction: a cluster analysis from the Eocene Gulf Coast (Ocala Limestone). Palaios, 420-423.

Naeher, S., Gilli, A., North, R.P., Hamann, Y., Schubert, C.J., 2013. Tracing bottom water oxygenation with sedimentary Mn/Fe ratios in Lake Zurich, Switzerland. Chemical Geology 352, 125-133.

Onac, B.P., Fornós, J., Merino, A., Ginés, J., Diehl, J., 2014. Linking mineral deposits to speleogenetic processes in Cova des Pas de Vallgornera (Mallorca, Spain). International Journal of Speleology 43, 4.

Onac, B.P., Mylroie, J.E., White, W.B., 2001. Mineralogy of cave deposits on San Salvador Island, Bahamas. Carbonates and Evaporites 16, 8-16.

Onac, B.P., Pedersen, R.B., Tysseland, M., 1997. Presence of rare-earth elements in black ferromanganese coatings from Vântului Cave (Romania). Journal of Caves and Karst Studies 59, 128-131.

Opsahl, S.P., Chanton, J.P., 2006. Isotopic evidence for methane-based chemosynthesis in the Upper Floridan aquifer food web. Oecologia 150, 89-96.

Opsahl, S.P., Chapal, S.E., Wheeler, C.C., 2005. Using stream gage data to quantify surface water/groundwater exchanges between the Upper Floridan aquifer and the lower Flint River, Georgia, USA, 1989-2003.

Panno, S.V., Curry, B.B., Wang, H., Hackley, K.C., Liu, C., Lundstrom, C., Zhou, J., 2004. Climate change in southern Illinois, USA, based on the age and δ13C of organic matter in cave sediments. Quaternary Research 61, 301-313.

Pham, A.N., Rose, A.L., Feitz, A.J., Waite, T.D., 2006. Kinetics of Fe (III) precipitation in aqueous solutions at pH 6.0–9.5 and 25 C. Geochimica et cosmochimica acta 70, 640-650.

Pohlman, J.W., Iliffe, T.M., Cifuentes, L.A., 1997. A stable isotope study of organic cycling and the ecology of an anchialine cave ecosystem. Mar Ecol Prog Ser 155, 17-27.

Polk, J.S., van Beynen, P.E., Asmerom, Y., Polyak, V., 2013. Reconstructing past climates using carbon isotopes from fulvic acids in cave sediments. Chemical Geology 360-361, 1-9.

Puri, H., 1964. Stratigraphy and zonation of the Ocala Group: Florida Geological Survey Bulletin 38, 248 p., and Vernon. RO.

Quade, J., Mifflin, M.D., Pratt, W.L., McCoy, W., Burckle, L., 1995. Fossil spring deposits in the southern Great Basin and their implications for changes in water-table levels near Yucca Mountain, Nevada, during Quaternary time. Geological Society of America Bulletin 107, 213-230.

Reimer, P.J., Bard, E., Bayliss, A., Beck, J.W., Blackwell, P.G., Ramsey, C.B., Buck, C.E., Cheng, H., Edwards, R.L., Friedrich, M., 2013. IntCal13 and Marine13 radiocarbon age calibration curves 0–50,000 years cal BP. Radiocarbon 55, 1869-1887.

Rose, A.L., Waite, T.D., 2003. Kinetics of hydrolysis and precipitation of ferric iron in seawater. Environmental science & technology 37, 3897-3903.

Schmidt, W., 1984. Neogene stratigraphy and geologic history of the Apalachicola embayment, Florida. State of Florida, Department of Natural Resources, Division of Resource Management, Bureau of Geology.

Schmidt, W., 1988. Florida Caverns State Park, Jackson County, Florida, Open File Report 23. Florida Geological Survey, Tallahassee, FL.

Schwertmann, U., Murad, E., 1983. Effect of pH on the formation of goethite and hematite from ferrihydrite. Clays and Clay Minerals 31, 277-284.

Spiteri, C., Regnier, P., Slomp, C.P., Charette, M.A., 2006. pH-Dependent iron oxide precipitation in a subterranean estuary. Journal of geochemical exploration 88, 399-403.

Stone, A.T., 1997. Reactions of extracellular organic ligands with dissolved metal ions and mineral surfaces. Reviews in mineralogy and Geochemistry 35, 309-344.

Survey, F.G., Scott, T.M., Anderson, D., 2001. Geologic map of the State of Florida. Florida Geological Survey.

Trombe, F., Fage, L., 1952. Traité de spéléologie. Payot Paris.

Van Breemen, N., 1988. Long-term chemical, mineralogical, and morphological effects of iron-redox processes in periodically flooded soils, Iron in soils and clay minerals. Springer, pp. 811-823.

van Hengstum, P.J., Donnelly, J.P., Toomey, M.R., Albury, N.A., Lane, P., Kakuk, B., 2014. Heightened hurricane activity on the Little Bahama Bank from 1350 to 1650 AD. Continental Shelf Research 86, 103-115.

van Hengstum, P.J., Reinhardt, E.G., Beddows, P.A., Gabriel, J.J., 2010. Investigating linkages between Holocene paleoclimate and paleohydrogeology preserved in Mexican underwater cave sediments. Quaternary Science Reviews 29, 2788-2798.

van Hengstum, P.J., Reinhardt, E.G., Beddows, P.A., Schwarcz, H.P., Garbriel, J.J., 2009. Foraminifera and testate amoebae (thecamoebians) in an anchialine cave: surface distributions from Aktun Ha (Carwash) cave system, Mexico. Limnology and Oceanography 54, 391-396.

van Hengstum, P.J., Richards, D.A., Onac, B.P., Dorale, J.A., 2015. Coastal caves and sinkholes, in: Shennan, I., Long, A.J., Horton, B.P. (Eds.), Handbook of Sea-level Research. John Wiley and Sons.

van Hengstum, P.J., Scott, D.B., 2012. Sea-level rise and coastal circulation controlled Holocene groundwater development and caused a meteoric lens to collapse 1600 years ago in Bermuda. Marine Micropaleonology 90-91, 29-43.

van Hengstum, P.J., Scott, D.B., Gröcke, D.R., Charette, M.A., 2011. Sea level controls sedimentation and environments in coastal caves and sinkholes. Marine Geology 286, 35-50.

Vinther, B.M., Clausen, H.B., Fisher, D., Koerner, R., Johnsen, S.J., Andersen, K.K., Dahl-Jensen, D., Rasmussen, S.O., Steffensen, J.P., Svensson, A., 2008. Synchronizing ice cores from the Renland and Agassiz ice caps to the Greenland Ice Core Chronology. Journal of Geophysical Research: Atmospheres (1984–2012) 113.

Watts, W., 1980. The late Quaternary vegetation history of the southeastern United States. Annual Review of Ecology and Systematics, 387-409.

Watts, W., Hansen, B., Grimm, E., 1992. Camel Lake: A 40 000-yr record of vegetational and forest history from northwest Florida. Ecology, 1056-1066.

Watts, W.A., 1969. A pollen diagram from Mud Lake, Marion County, North-Central Florida. Geological Society of America Bulletin 80, 631-642.

Watts, W.A., Hansen, B.C., 1988. Environments of Florida in the late Wisconsin and Holocene. Wet site archaeology, 307-323.

Watts, W.A., Hansen, B.C.S., 1994. Pre-Holocene and Holocene pollen records of vegetation history from the Florida peninsula and their paleoclimatic implications. Palaeogeography, Palaeoclimatology, Palaeoecology 109, 163-176.

Watts, W.A., Stuiver, M., 1980. Late Wisconsin climate of northern Florida and the origin of species-rich deciduous forest. Science 210, 325-327.

White, W.A., 1970. The geomorphology of the Florida peninsula.

White, W.B., 2007. Cave sediments and paleoclimate. Journal of Cave and Karst Studies 69, 76-93.

Wickert, A.D., Mitrovica, J.X., Williams, C., Anderson, R.S., 2013. Gradual demise of a thin southern Laurentide ice sheet recorded by Mississippi drainage. Nature 502, 668-671.

Winkler, M., Sanford, P., Kaplan, S., 2001. Hydrology, vegetation, and climate change in the southern Everglades during the Holocene. Bulletins of American Paleontology, 57-100.

Wurster, C.M., Patterson, W.P., McFarlane, D.A., Wassenaar, L.I., Hobson, K.A., Beavan-Athfield, N., Bird, M.I., 2008. Stable carbon and hydrogen isotopes from bat guano in the Grand Canyon, USA, reveal Younger Dryas and 8.2 ka events. Geology 36, 683-686.

Yamamoto, N., Kitamura, A., Irino, T., Kase, T., Ohashi, S., 2010. Climatic and hydrologic variability in the East China Sea during the last 7000 years based on oxygen isotopic records of the submarine caverniculous micro-bivalve *Carditella iejimensis*. Global Planetary Change 72, 131-140.

Yamamoto, N., Kitamura, A., Ohmori, A., Morishima, Y., Toyofuku, T., Ohashi, S., 2009. Long-term changes in sediment type and cavernicolous bivalve assemblages in Daidokutsu submarine cave, Okinawa Islands: evidence from a new core extending over the past 7,000 years. Coral Reefs 28, 967-976.

Zarikian, C.A.A., Swart, P.K., Gifford, J.A., Blackwelder, P.L., 2005. Holocene paleohydrology of Little Salt Spring, Florida, based on ostracod assemblages and stable isotopes. Palaeogeography, Palaeoclimatology, Palaeoecology 225, 134-156.